A Desalination Battery

Mauro Pasta,[†] Colin D. Wessells,[‡] Yi Cui,[‡,§] and Fabio La Mantia[†,*]

[†]Analytische Chemie — Zentrum für Elektrochemie, Ruhr-Universität Bochum, Universitätsstrasse 150, D-44780 Bochum, Germany
[‡]Department of Materials Science and Engineering, Stanford University, Stanford, California 94305, United States
[§]Stanford Institute for Materials and Energy Sciences, SLAC National Accelerator Laboratory, 2575 Sand Hill Road, Menlo Park, California 94025, United States

Ⓢ Supporting Information

ABSTRACT: Water desalination is an important approach to provide fresh water around the world, although its high energy consumption, and thus high cost, call for new, efficient technology. Here, we demonstrate the novel concept of a "*desalination battery*", which operates by performing cycles in reverse on our previously reported mixing entropy battery. Rather than generating electricity from salinity differences, as in mixing entropy batteries, desalination batteries use an electrical energy input to extract sodium and chloride ions from seawater and to generate fresh water. The desalination battery is comprised by a $Na_{2-x}Mn_5O_{10}$ nanorod positive electrode and Ag/AgCl negative electrode. Here, we demonstrate an energy consumption of 0.29 Wh l[−1] for the removal of 25% salt using this novel desalination battery, which is promising when compared to reverse osmosis ($\sim$ 0.2 Wh l[−1]), the most efficient technique presently available.

KEYWORDS: Seawater desalination, mixing entropy battery, reverse osmosis, ion selectivity
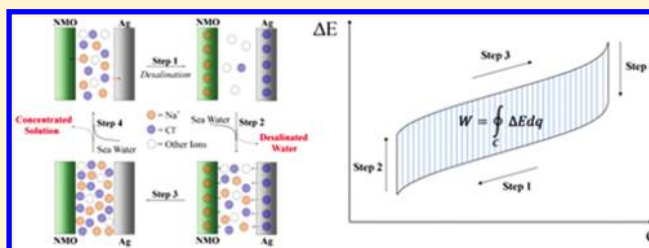
Increasing amounts of fresh water will be required in the future as a result of the increase in population and enhanced living standards, as well as the expansion of industrial and agricultural activities.[1,2] At the current growth rate, humans will consume 90% of available fresh water by 2025, by which time the population living in water-stressed areas is expected to increase to 3.9 billion.[3] Seawater desalination is becoming a feasible source for fresh water, free from local and global variations in rainfall. For this reason, the use of seawater desalination has steadily increased in recent years.

Seawater desalination processes require electric or thermal energy to separate saline seawater into two streams, a fresh water stream containing a low concentration of dissolved salts and a concentrated brine stream. A variety of desalination technologies have been developed over the years.[2,4−10] Reverse osmosis requires a large electrical energy input, which accounts for 44% of its cost,[1] and it is based on selective membranes, which are prone to fouling and require frequent replacement.[11] Recent research on high-flux membranes based on carbon nanotubes[12] could potentially reduce the energy consumption, while alternative electrical-based desalination technology such as ion concentration polarization in nanodevices[13] can potentially avoid the fouling.

Thermal energy based multistage flash distillation requires energy intensive heating to temperatures above 90 °C, accounts for 50% of its cost.[1] Multiple effect distillation is gaining popularity due to its higher efficiency and lower top brine temperatures (about 70 °C) than multistage flash technology.[14] Forward osmosis is a promising new process that utilizes lower

temperatures (60 °C) but still requires the use of membranes.[15,16] Solvent extraction using directional solvents like decanoic acid at mild temperatures (30−50 °C) has been demonstrated recently by Bajpayee and co-workers.[3] Previous electrochemical approaches relying on the electrical double-layer built at the surface of high surface area carbonaceous electrodes are capacitive deionization (CDI)[17] and the newly developed capacitive double layer expansion (CDLE).[18,19] Despite these recent advances, the 50−80% target for reduction in desalination costs by 2020 set by the National Research Council roadmap will not be achieved by incremental improvements to existing technologies, and therefore, a new approach is needed.[1]

Here we introduce a new concept of a "desalination battery" which is based on a previously described device known as the "mixing entropy battery".[20] This desalination battery operates in a similar way to the capacitive desalination techniques[21] but instead of storing charge in the electrical double layer (built at the surface of the electrode) it is held in the chemical bonds (bulk of the electrode material). Battery electrodes offer higher specific capacity and lower self-discharge than capacitive electrodes.[22]
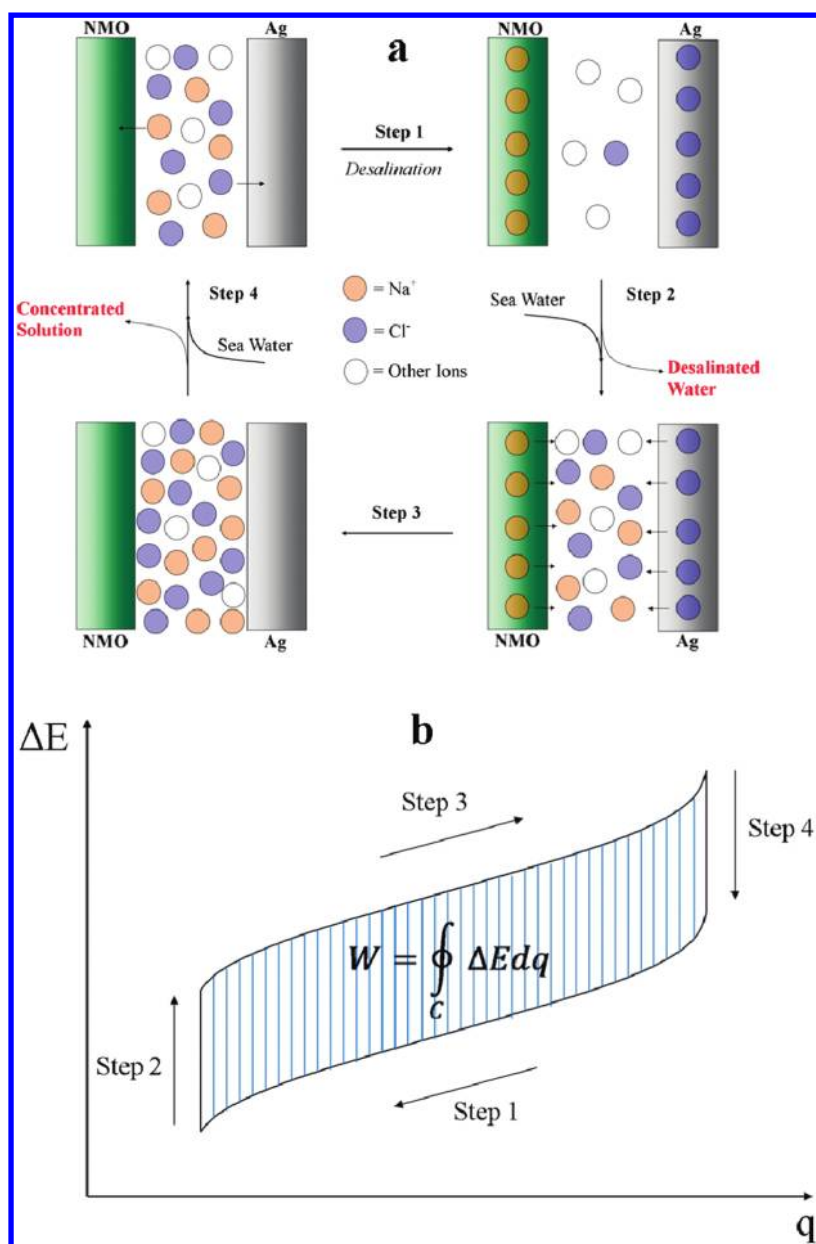
In this work, we reversed the previously proposed four step cycle of the mixing entropy battery, in a fashion similar to the four cycles of the CDI and CDLE. This desalination battery

Figure 1. (a) Schematic representation of the working principle behind a complete cycle of the desalination battery, showing how energy extraction can be accomplished: step 1, desalination; step 2, removal of the desalinated water and inlet of sew water; step 3, discharge of Na$^+$ and Cl$^-$ in seawater; step 4, exchange to new seawater. (b) Typical form of a cycle of battery cell voltage (ΔE) vs charge (q) in the desalination battery, demonstrating the energy consumed.

consists of a cationic sodium insertion electrode and a chloride-capturing anionic electrode. A four-step charge/discharge process allows these electrodes to separate seawater into fresh water and brine streams. In the first step, the fully charged electrodes, which do not contain mobile sodium or chloride ions when charged, are immersed in seawater. A constant current is then applied in order to remove the ions from the solution (Figure 1, Step 1). In the second step (Figure 1, Step 2), the fresh water solution in the cell is extracted and then replaced with additional seawater. The electrodes are then recharged in this solution, releasing ions and creating brine (Figure 1, Step 3). In the final, fourth step (Figure 1, Step 4), the brine solution is replaced with new seawater, and the desalination battery is ready for the next cycle. Fresh water is produced during the initial discharge of the electrodes (Steps 1−2), while recharging the electrodes results in the production

of a brine stream (Steps 3−4). Figure 1b schematically shows a typical potential profile of a desalination battery as a function of charge state. The circular integral of this curve is equal to the net amount of electrical energy needed to drive the desalination of the seawater.[23]

To demonstrate the validity of our desalination battery design, electrochemical cell employing the following reaction were constructed

$$5MnO_2 + 2Ag + 2NaCl \leftrightarrow Na_2Mn_5O_{10} + 2AgCl$$
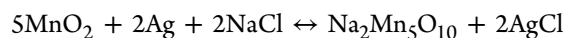
An electrode made of Na$_{2-x}$Mn$_5$O$_{10}$ (NMO) nanorods[20] was used to capture Na$^+$ ions, and a Ag electrode was used to capture Cl$^-$ ions (see Supporting Information for detailed electrode preparation). Among the few good water compatible Na$^+$ insertion materials now available, we selected Na$_2$Mn$_5$O$_{10}$

because of its higher specific charge storage capacity (35 mAh g^{-1}), low cost, and benign environmental impact.[24,25] Identifying a suitable electrode for chloride capture is more difficult. Silver has been used because it forms AgCl, by capturing chloride ions, which is stable in potential and is insoluble.

The NMO has been prepared by a "polymer synthesis method",[26] with which nanorods with a mean diameter of 300 nm and length of about 2 μm were obtained (Figure 2a-b). The
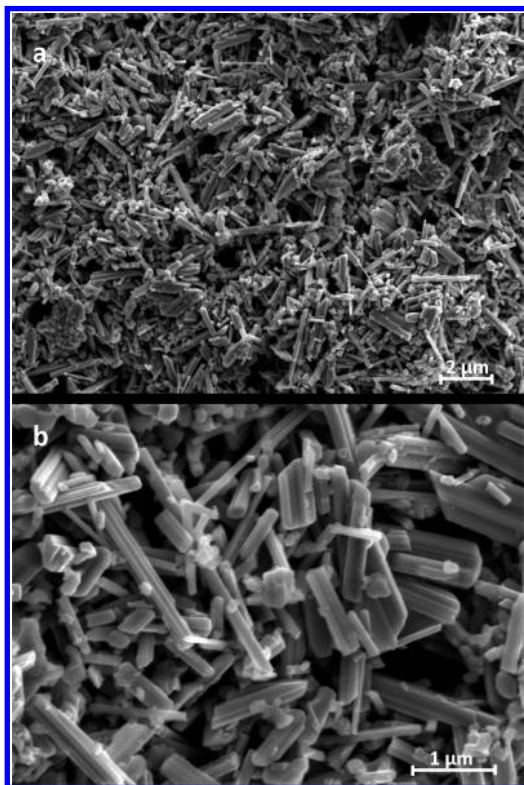
Figure 2. SEM images of the as-prepared $Na_2Mn_5O_{10}$ showing (a) good uniformity of nanorod morphology throughout the sample, and (b) nanorods with an average size about 300 nm in width and 1−3 μm in length.

nanoscale morphology of the NMO results in the exposure of a high surface area to the solution, and therefore, fast exchange of ions between the solid and the liquid phase occurs. Also, the short diffusion length within the individual NMO nanorods permits a fast transfer of sodium ions from their surfaces into their bulk interiors. The NMO electrode was then prepared by drop casting a NMO-based ink on a carbon cloth current collector; these electrodes showed typical electrochemical behavior when in contact with sodium containing electrolytes.[24,27] A similar approach was used for the Ag electrode, and in this case the ink contained silver microparticles (0.5−1.0 μm diameter). The choice of a carbon cloth current collector is dictated by its corrosion resistance in highly saline seawater. In addition, the superior adherence and soaking of the ink into the carbon fibers results in higher mass loading, improving device performance. The as-prepared $Na_2Mn_5O_{10}/AgCl$ cell was subjected to galvanostatic cycling in an aqueous solution containing 0.6 M NaCl in order to evaluate the optimal operational potential range (Figure 3a). Three reaction plateaus are observed at 0.3, 0.6, and 1.0 V, and each one of them corresponds to the intercalation of Na^+ into a crystallo-
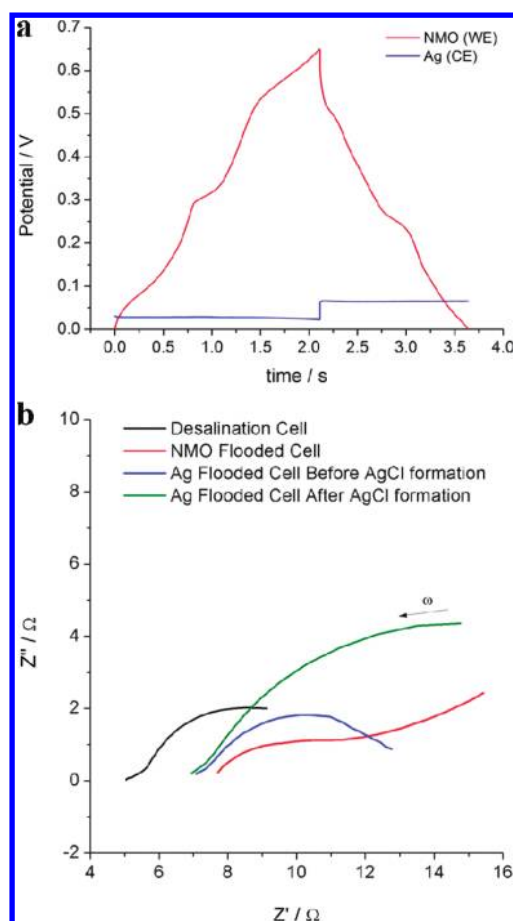
Figure 3. (a) Galvanostatic (1 mA) cycling of the $Na_2Mn_5O_{10}$ (WE)− Ag (CE) system versus Ag/AgCl/KCl 3M. (b) Nyquist plot of the EIS spectra in the frequency range 100 kHz to 1 Hz of: NMO working electrode (red curve), silver counter electrode before (blue curve) and after (green curve) chloride formation in a in seawater electrolyte with a three electrode setup. Black curve is the spectra of the desalination cell.

graphically distinct site in the NMO structure. The reaction plateau at 0.3 V is most desirable for use in a desalination battery because it is highly reversible with little self-discharge and has a low enough potential to avoid oxygen gas evolution in pH-neutral electrolytes such as seawater.

Electrochemical impedance spectroscopy (EIS) was used to identify the limiting step in the electrochemical reactions occurring in the cell. As shown in Figure 3b, it is evident that the formation of AgCl on the surface of the silver microparticles substantially increases the impedance of the system. In contrast, the NMO electrode, which has a high surface area, has a small charge transfer resistance, and is diffusion-limited. It is not possible to address through these measurements whether or not the diffusion control is due to the solution or to the solid state. The resistance of the solution in the desalination cell is more than 50% lower than in the flooded cell due to the positioning of the electrodes.

Desalination battery cycling was performed in a custom-made plexiglass cell (see Supporting Information). The cell permits only a two-electrode geometry, with three compartments, two for the two electrodes, and one for the electrolyte. The total volume of the cell is around 300 μL, and it exposes to the solution 2 cm^2 of the electrodes. This cell geometry has the

advantage of a reduced ohmic drop and minimal processed volume.

The desalination cycle is started with the electrode materials in their charged state in seawater. During the first step a -500 μA cm^{-2} current is applied, and ions are removed from the solution. Through control of the total discharge, the quantity of ions removed can be controlled. The desalinated solution was then removed from the cell and replaced with new seawater (Step 2). Then the desalinated solution was analyzed by ICP-MS in order to evaluate the Coulombic efficiency of the desalination process (Table 1). In the third step, a $+500$ μA

Table 1. ICP-OES/ICP-MS: Coulombic Efficiencies and Selectivity for Anions and Cations

ion	Na$^+$	K$^+$	Mg^{2+}	Ca^{2+}	Cl$^-$	SO$_4^{2-}$
sea water (mg/L)	11250	450	1400	450	18500	2750
25% removal (mg/L)	9840	430	1130	280	14470	2750
$\eta_{C,25}$	47%	<1%	9%	3%	87%	control
50% removal (mg/L)	7860	390	860	180	11430	2750
$\eta_{C,50}$	57%	<1%	9%	3%	76%	control

cm^{-2} current is applied, charging the electrodes by releasing the ions incorporated in the first step. The resulting concentrated seawater solution is then replaced with new seawater (Step 4), completing the cycle; the system is then ready for the further cycling.

The cycle for a 25% removal of chlorides is reported in Figure 4. The circular integral of the E vs Q curve represents
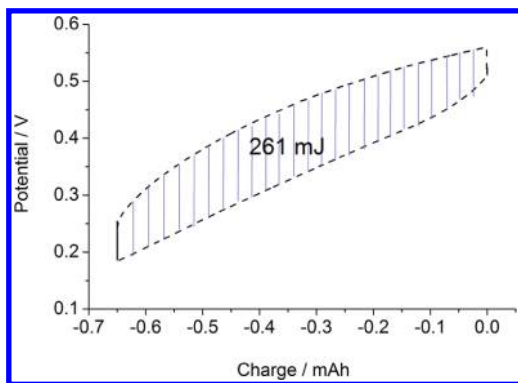
Figure 4. Desalination cycle in real seawater for 25% removal of NaCl. The energy consumption is represented by the path integral of the ΔE vs q curve.

the energy required for the desalination process (removal of 25% of salt) to take place, which is on the order of 0.29 Wh l^{-1}. This value is very promising when compared to the reverse osmosis under similar conditions (0.2 Wh l^{-1}).[13] In Table 1, the results of the ICP-MS analysis of the seawater and the desalinated seawater are reported for a theoretical removal of 25 and 50% of chlorides, respectively. To address uncertainty in the extracted volume from the desalination cell, sulfate ions were used as a control in the experiment. Sulfate ions cannot be removed by using silver because Ag$_2$SO$_4$ is formed only at high voltages (0.65 V/NHE) that are never achieved in the desalination cell. All of the other concentrations were obtained by bringing the concentration of sulfate ions equal to that in seawater. The Coulombic efficiencies, η_C, reported in Table 1

are defined as

$$\eta_{C,i} = \frac{z_i F (n_I - n_F)}{Q}$$

where z_i is the valence state of the ion, F is the Faraday constant, n_I and n_F are the initial and final number of moles in the solution, and Q is the total charge flown. Coulombic efficiencies, which should not be confused with the energy efficiency of the device, provide information regarding the selectivity of the electrode material toward the ions in solution. In fact, it is notable that the extraction of cations is not Na$^+$ selective but also Ca^{2+}, Mg^{2+}, and K$^+$ are able to insert in the NMO structure. Comparison of the crystal ionic radii of these cations shows that Ca^{2+} and Na$^+$ have a very similar radius (around 115 pm), Mg^{2+} is smaller (around 86), while K$^+$ is clearly bigger (ca. 150 pm). As consequence of this, it is observed (Table 1) that calcium, magnesium, and sodium are also removed from seawater, while potassium is removed to a lesser extent. The total Coulombic efficiency of the desalination can be obtained from the value of chlorides and is ca. 80%. The remaining charge (about 20%) is lost during the reduction of oxygen and formation of OH$^-$.

The desalination battery has simple construction, uses readily available materials, has a promising energy efficiency, operates at room temperature with fewer corrosion problems than existing desalination technology, and it could potentially be Na$^+$ and Cl$^-$ selective, which would end the need for resalination. Its primary limitation of low total ion extraction arises from the low specific charge capacity of the NMO sodium ion electrode (35 mAh g^{-1} vs an average value of 160 mAh g^{-1} for Li-intercalating cathodes). This low charge capacity limits the volume of water that can be desalinated within one cycle, and therefore the overall efficiency of desalination. However, the battery research community has recently shown increasing interest in aqueous sodium ion batteries for grid scale power storage applications. In the near future, higher capacity sodium ion electrodes, as well as improved chloride electrodes will make the desalination battery a feasible method for seawater desalination. With regard to the chloride intercalation/ capturing electrode material, silver shows several advantages: stability of potential, corrosion resistance, and bactericidal properties. Nevertheless, the high price of silver, and poor electronic conductivity of AgCl, which is the primary kinetic limitation of the desalination battery (see Supporting Information) will limit the utility of the Ag/AgCl electrode in practical devices. The work reported here demonstrates the concept of a desalination battery. Further developments will result in a versatile technology for the desalination of seawater, either independently or through integration with other desalination methods.

■ ASSOCIATED CONTENT

Ⓢ Supporting Information
Additional information, figures, and table. This material is available free of charge via the Internet at http://pubs.acs.org.

■ AUTHOR INFORMATION

Corresponding Author
*E-mail: fabio.lamantia@rub.de.

■ ACKNOWLEDGMENTS

■ REFERENCES

(1) National Academies Press 2004.

(2) Khawaji, A. D.; Kutubkhanah, I. K.; Wie, J.-M. *Desalination* **2008**, *221* (1−3), 47−69.

(3) Bajpayee, A.; Luo, T.; Muto, A.; Chen, G. *Energy Environ. Sci.* **2011**, *4*, 1692.

(4) Howe, E. D. Fundamentals of Water Desalination. In *Environmental Science and Technology Series*; Dekker: New York, 1974; Vol. *1*, p 360.

(5) Buros, O. K. *J. Am. Water Works Assoc.* **1989**, *81*, 38−42.

(6) *Principles of Desalination*, 2nd ed; Spiegler, K. S., Laird, A. D. K., Eds.; Academic Press: New York, 1980; Part A, p 357.

(7) *Principles of Desalination*, 2nd ed; Spiegler, K. S., Laird, A. D. K., Eds.; Academic Press: New York, 1980; Part b, p 463.

(8) *Desalination Technology: Developments and Practice*; Porteous, A., Ed.; Applied Science Publishers: London, 1983; p 271.

(9) Saline Water Processing. In *Desalination and Treatment of Seawater, Brackish Water, and Industrial Waste Water*; Heitmann, H. G., Ed.; VCH: New York, 1990; p 332.

(10) Van, d. B. B.; Vandecasteele, C. *Desalination* **2002**, *143*, 207−218.

(11) Shannon, M. A.; Bohn, P. W.; Elimelech, M.; Georgiadis, J. G.; Marinas, B. J.; Mayes, A. M. *Nature* **2008**, *452* (7185), 301−310.

(12) Holt, J. K.; Park, H. G.; Wang, Y.; Stadermann, M.; Artyukhin, A. B.; Grigoropoulos, C. P.; Noy, A.; Bakajin, O. *Science* **2006**, *312* (5776), 1034−1037.

(13) Kim, S. J.; Ko, S. H.; Kang, K. H.; Han, J. *Nat. Nanotechnology* **2010**, *5* (4), 297−301.

(14) Ophir, A.; Lokiec, F. *Desalination* **2005**, *182* (1−3), 187−198.

(15) McCutcheon, J. R.; McGinnis, R. L.; Elimelech, M. *Desalination* **2005**, *174* (1), 1−11.

(16) Cath, T. Y.; Childress, A. E.; Elimelech, M. *J. Membr. Sci.* **2006**, *281*, 70−87.

(17) Arnold, B. B.; Murphy, G. W. *J. Phys. Chem.* **1961**, *65* (1), 135−138.

(18) Brogioli, D. *Phys. Rev. E* **2011**, *84* (3), 031931.

(19) Brogioli, D.; Zhao, R.; Biesheuvel, P. M. *Energy Environ. Sci.* **2011**, *4* (3), 772−777.

(20) La Mantia, F.; Pasta, M.; Deshazer, H. D.; Logan, B. E.; Cui, Y. *Nano Lett.* **2011**, *11* (4), 1810−1813.

(21) Brogioli, D. *Phys. Rev. Lett.* **2009**, *103* (5), 058501/1−058501/4.

(22) Conway, B. E. *J. Electrochem. Soc.* **1991**, *138* (6), 1539−48.

(23) Biesheuvel, P. M. *J. Colloid Interface Sci.* **2009**, *332* (1), 258−264.

(24) Tevar, A. D.; Whitacre, J. F. *J. Electrochem. Soc.* **2010**, *157* (7), A870−A875.

(25) Sauvage, F.; Laffont, L.; Tarascon, J. M.; Baudrin, E. *Inorg. Chem.* **2007**, *46* (8), 3289−3294.

(26) Deshazer, H. D.; La Mantia, F.; Wessels, C.; Huggins, R. A.; Cui, Y. *Nano Lett.* **2011**, *11* (4), 1810−1813.

(27) Whitacre, J. F.; Tevar, A.; Sharma, S. *Electrochem. Commun.* **2010**, *12* (3), 463−466.